

Supplementary Information

Electrochemiluminescence Sensor for Dopamine with the Dual Molecular Recognition Strategy Based on Graphite-like Carbon Nitride Nanosheets/3,4,9,10-Perylenetetracarboxylic Acid Hybrids

Xiaomin Fu^a, Jiahui Feng^a, Xingrong Tan^b, Qiyi Lu^a, Ruo Yuan^a and Shihong Chen^{a*}

^a*Key Laboratory of Luminescent and Real-Time Analytical Chemistry (Southwest University) , Ministry of Education, College of Chemistry and Chemical Engineering, Southwest University, Chongqing 400715, China*

^b*Department of Endocrinology, 9 th People's Hospital of Chongqing, Chongqing 400700, China*

E-mail address: cshong@swu.edu.cn. (S. Chen)

Table S1 Comparison of the prepared ECL sensor with different reported sensors for the determination of DA.

Table S2 Recoveries test of DA in hydrochloride injection sample.

Table S3 The ECL signal of the blank for twelve times.

Fig. S1 CVs of (A) the g-C₃N₄ NSs-PTCA/mercaptan/APTES/AuNPs/GCE electrode and (B) the g-C₃N₄ NSs-PTCA/DA/mercaptan/APTES/AuNPs/GCE electrode in the absence (a) and in the presence (b) of 3.0×10⁻⁹ M DA in 0.10 M PBS (pH 7.0). CV mode was performed with potential scanning from 0 to 0.6 V. Scan rate: 100 mV s⁻¹.

Fig. S2 The ECL stability of the sensor to 0.3 nM DA in 0.10 M PBS (pH 7.0)

containing 0.10 M $K_2S_2O_8$.

Fig. S3 The storage stability of the sensor.

Fig. S4 The ECL response of the sensor to 3.0 nM (a) KCl, (b) Na_2SO_4 , (c) ascorbic acid, (d) tyrosine, (e) glucose, (f) ascorbic acid, (g) epinephrine and (h) clenbuterol, respectively. Column j is the ECL response of the sensor toward 0.3 nM DA.

Fig. S5 The structure of epinephrine (a), clenbuterol (b) and DA (c).

Fig. S6 Calibration plots at a low concentration range of DA.

Table S1

Electrode	Method	Linear response range (mol L ⁻¹)	Limit of detection (mol L ⁻¹)	Reference
rGO/MWCNTs/AuNPs/GCE	ECL	$2.0 \times 10^{-7} \sim 7 \times 10^{-5}$	6.7×10^{-8}	1
Ru(bpy) ₃ ²⁺ /OMC@Nafion/GCE	ECL	$5.0 \times 10^{-9} \sim 5.0 \times 10^{-4}$	7.0×10^{-9}	2
CNTs/P1 ^c /DA/DSP-QDs ^d	ECL	$5.0 \times 10^{-11} \sim 1.0 \times 10^{-8}$	2.6×10^{-11}	3
PNVs ^e /GCE	ECL	$1.0 \times 10^{-11} \sim 2.0 \times 10^{-10}$	3.15×10^{-12}	4
PEI-MWNTs-AuNPs/GCE	DPV ^a	$5.0 \times 10^{-8} \sim 4.0 \times 10^{-6}$	6.56×10^{-9}	5
Ppy-RGO /GCE	DPV	$1.0 \times 10^{-8} \sim 1.0 \times 10^{-5}$	1.0×10^{-9}	6
Porous carbon/GCE	CV ^b	$9.0 \times 10^{-9} \sim 3.0 \times 10^{-7}$	2.9×10^{-9}	7
AuNF@g-C ₃ N ₄ -PANI/GCE	ECL	$5.0 \times 10^{-9} \sim 1.6 \times 10^{-6}$	1.7×10^{-9}	8
PTC-NH ₂ /GCE	ECL	$5.0 \times 10^{-9} \sim 1.1 \times 10^{-6}$	1.6×10^{-9}	9
g-C ₃ N ₄ -PTCA/DA/APTES/AuNPs/GCE	ECL	$3.0 \times 10^{-12} \sim 6 \times 10^{-9}$	2.4×10^{-12}	This work

^aDPV, differential pulse voltammetry.

^bCV, cyclic voltammetric profiles.

P1^c, a boronic acid-functionalized pyrene probe

DSP-QDs^d, 3,3'- dithiodipropionic acid di(N-hydroxysuccinimide ester) (DSP)-functionalized CdTe QDs

PNVs^e, peptide nanovesicles

Table S2

Sample	C_{original} (nM)	C_{Added} (nM)	C_{Detected} (nM) ^a	Recovery (%)	RSD (%)
1	0.020	1.02	1.07±0.05	103	4.7
2	0.020	0.167	0.198±0.003	107	1.5
3	0.020	0.033	0.052±0.001	97.0	1.9
4	0.020	0.017	0.036±0.001	94.1	2.8

^a Mean ± SD, $n = 3$.

Table S3

Number	1	2	3	4	5	6
<i>I</i> / a.u	23	19	22	25	25	22
Number	7	8	9	10	11	12
<i>I</i> / a.u	22	22	24	22	24	24

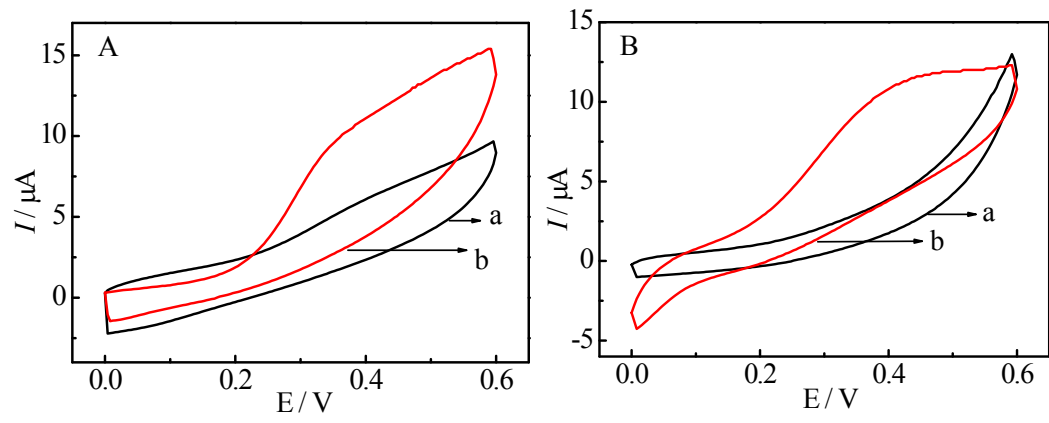


Fig. S1

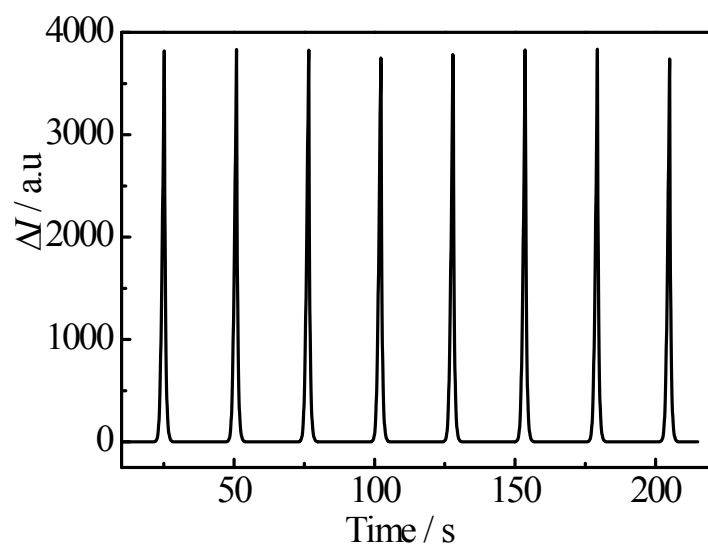


Fig. S2

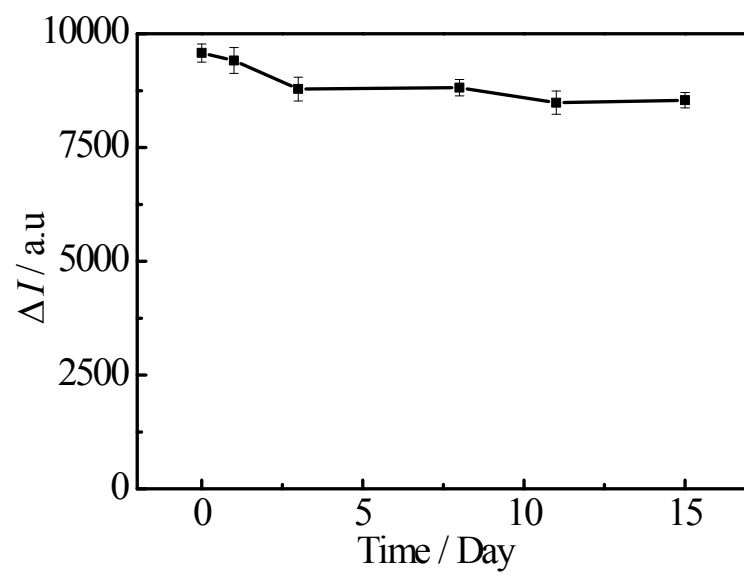


Fig. S3

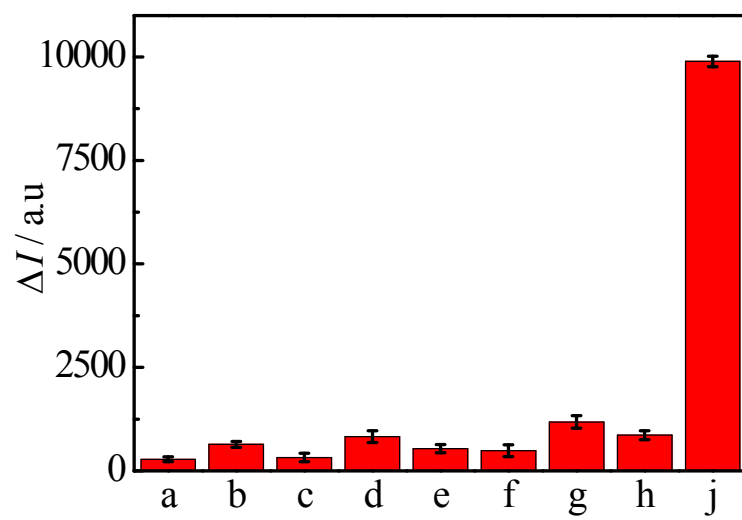


Fig. S4

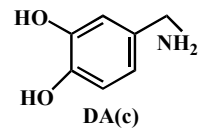
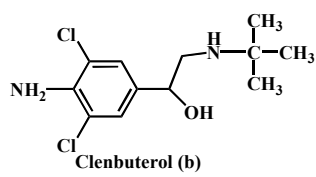
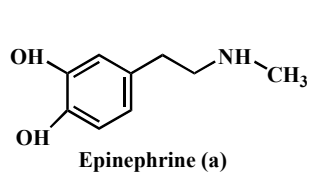


Fig .S5

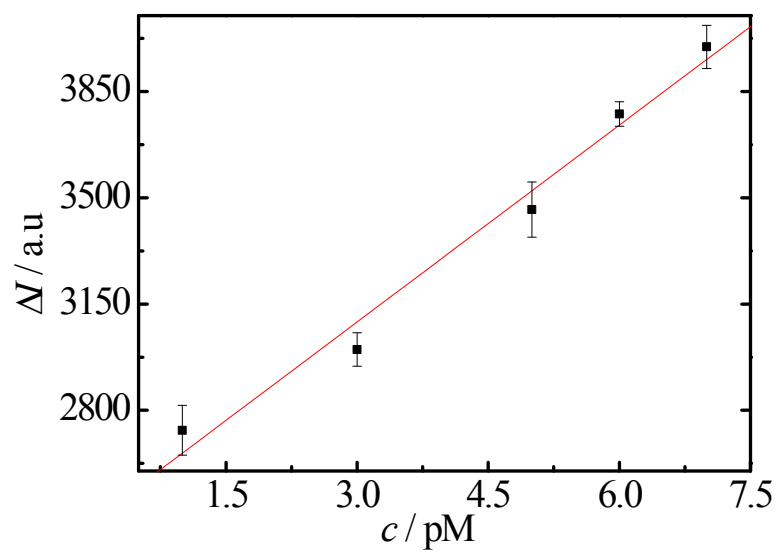


Fig. S6

As for the detection limit (LOD), it was calculated according to the IUPAC recommendation ⁹

$$\text{LOD} = k S_b / m$$

Here, k is the numerical factor chosen in accordance with the desired confidence level. As suggested by Long and Winefordner,¹⁰ the use of $k = 3$ allows a confidence level of 99.86% for a normal distribution of the blank signals. S_b is the standard deviation of the blank signals ($n_B=12$), and m is the analytical sensitivity, which can be estimated by the slope of calibration plot at lower concentration ranges. Fig. S6 displayed the calibration curve between ΔI and DA concentration at lower concentration ranges of DA. The corresponding calibration equation was $\Delta I = 2.16 c_{\text{pM}} + 2442.5$.

The S_b of twelve times zero-dose was 1.7, and the detailed data were presented in Table S3. In addition, relative standard deviation (RSD) of 7.4% for twelve times was obtained. Therefore, the recalculated LOD of the proposed sensor according to IUPAC recommendation is 2.4 pM ($\text{LOD} = 3 \times 1.7 \div 2.16 = 2.4$).

Limit of detection (LOQ) was calculated using the equations: $\text{LOD} = 10 S_b / m$,¹¹ and 7.9 pM of LOQ was obtained.

References

1. D. H. Yuan, S. H. Chen, R. Yuan, J. J. Zhang, X. F. Liu, *Sensors Actuat B-Chem.*, 2014, **191**, 415–420.
2. B. N. Wu, , C. C. Miao, L. L. Yu, Z. Y. Wang, C. S. Huang, N. Q. Jia, *Sensors Actuat B-Chem.*, 2014,**195**, 22–27.
3. L. Zhang, Y. Cheng, J. P. Lei, Y. T. Liu, Q. Hao, H. X. Ju, *Anal. Chem.*, 2013, **85**, 8001–8007
4. C. X. Huang, X. Chen, Y. L. Lu, H. Yang, W. S. Yang, *Biosens. Bioelectron.*, 2015, **63**, 478–482.
5. L.Y. Jin, X. Gao, L. S. Wang, Q. Wu, Z. C. Chen, X. F. Lin, *J Electroanal Chem.*, 2013, **692**, 1–8
6. T. Qian, S. S. Wu, J. Shen, *Chem. Commun.*, 2013, **49**, 4610–4612.
7. P. Veerakumar, R. Madhu, S. M. Chen, C. T. Hung, P. H. Tang, C. B. Wang, S. B. Liu, *Analyst.*, 2014, **139**, 4994–5000.
8. Q. Y. Lu, J. J. Zhang, X. F. Liu Y. Y. Wu, R. Yuan, S. H. Chen, *Analyst.*, 2014, **139**, 6556–6562.
9. IUPAC, *Pure Appl. Chem.*, 1976, **45**, 107.
10. G. L. Long, J. D. Winefordner, *Anal. Chem.*, 1983, **55**, 712A-724A.
11. S. S. Kalanur, J. Seetharamappa, S.N. Prashanth., *Colloid Surface B*, 2010, **78** 217–221